Features extraction from cardiac-related signals: comparison among different measurement methods

Features extraction from cardiac-related signals: comparison among different measurement methods

G. Cosoli, G.M. Revel, L. Scalise

Department of Industrial Engineering and Mathematical Sciences, Università Politecnica delle Marche, v. Brecce Bianche snc, 60131 Ancona (Italy)

g.cosoli@staff.univpm.it, 0000-0001-7982-208X

Abstract. Heart Rate (HR), Heart Rate Variability (HRV), and cardiac time intervals are clinically relevant parameters, which can be assessed from the analysis of electrocardiogram (ECG). Some aspects of cardiac activity can be investigated also by means of different non-invasive and non-intrusive measurement methods, such as phonocardiograph (PCG), photoplethysmograph (PPG), and vibrocardiograph (VCG). However, the standard processing algorithms (i.e., Pan & Tompkins) do not allow to fully characterize waveforms different from ECG. In the past, some of the authors have already demonstrated the efficiency of a novel processing procedure for the precise HR measurement from the above-mentioned signals. In the present work, data processing procedure has been improved and deeply extended to assess HRV parameters and time intervals from all the signals acquired on an extended experimental campaign, involving 26 subjects, on whom ECG, PPG, PCG, and VCG signals were simultaneously measured. Results prove that this approach can overcome the drawbacks of standard algorithms and can be widely applied to signals of different nature to derive HR, HRV, and time intervals. As regards HR measurement, PPG proved to be the most accurate measurement method (±1.2 bpm), followed by VCG (±1.6 bpm) and PCG (±2.5 bpm). For HRV analysis in the time domain, the use of the proposed methodology allows to obtain clinically relevant parameters statistically comparable to the ECG ones. Finally, the measurement of QT interval by applying personal calibration lines allows to obtain results comparable to the gold standard technique, i.e., ECG (maximum percentage deviation reduced from 10.9% up to <4.3% in VCG).

1. Introduction

Heart Rate (HR) is a fundamental parameter to monitor a subject's health status [1], which can be affected by several conditions (e.g., anxiety, stress, or illness [2,3]). The automatic detection of cardiac peaks is fundamental not only for patient monitoring, but also in the healthcare context (i.e., monitoring out of hospitalization conditions [4,5]). According to Kranjec et al. [6], the HR measurement can be performed with "contact", "fixed-in-environment", and "non-contact" sensors [7]. The gold standard for HR measurement is electrocardiography (ECG). However, over the years other contact methods to monitor cardiac rhythm have been developed, such as Phonocardiography (PCG) and Photoplethysmography (PPG), also in wearable form [8–10]. Vibrocardiography (VCG) [11,12] is a non-contact method, which detects the vibrations of the skin surface resulting from vascular blood motion consequent to the electrical signal (ECG). In a standard ECG, both waves and time intervals are well known and of acknowledged physiological relevance (e.g., QT interval, which

represents the electrical depolarization and repolarization of ventricles [13]). More than this, several clinically relevant parameters can be obtained from Heart Rate Variability (HRV) analysis [14]. HRV can be seen as the natural variability of HR in response to internal or external stimuli, e.g., emotional states, stress, and relaxation. In a healthy cardiac system, the HR responds quickly to all these factors, so that the subjects' psychophysical adaptability is optimized. For the extraction of these parameters (i.e., HR, HRV, and time intervals), a dedicated algorithm is required. As regards ECG signal, the most widely used processing technique is based on Pan & Tompkins algorithm [15]. However, this methodology suffers from two main drawbacks: first, it allows the identification of the mere R-peak and not of the other characteristic points in the ECG waveform (i.e., P, Q, S, and T waves); moreover, it works only for ECG signal. For these reasons, a more robust and flexible algorithm is needed to overcome these limitations. Several algorithms are provided in literature for the identification of singular features in ECG signal. For example, techniques for the automatic detection and classification of QRS complexes are presented in [16,17], whereas Hossain et al. [18] detect also P wave. The algorithm proposed in [19] has been proved to be accurate for the identification of all the waves typical of ECG waveform, independently from the isoelectric segment. This aspect represents an advantage with respect to other algorithms, requiring a specific base-line correction [20]. Moreover, in their previous work [21], the authors have demonstrated the applicability of an improved version of this approach also to other physiological signals acquired by means of non-invasive measurement methods (i.e., PCG, PPG, and VCG).

In this work, the algorithm performance has been assessed not only in terms of HR measurement, but also concerning HRV parameters and cardiac time intervals. In particular, as regards HRV analysis, the authors have focused on the evaluation of the time domain parameters [14], by means of statistical Student's t-tests and their graphical representations through 95% Confidence Intervals (CI). Then, the agreement between QT time intervals computed from test signals (i.e., PPG, PCG, and VCG) and reference signal (i.e., ECG) has been evaluated.

Different types of main features can be identified for the considered signals:

- PCG signal: first sound (S1), corresponding to the atrioventricular valves closure (beginning of systole), and second sound (S2), related to the closure of aortic and pulmonary valves (end of systole) [22].
- PPG signal: main peak (P1), representing the blood volume variation due to pressure pulse.
- VCG signal: V1-peak – but also other points are identifiable [21], as well for PPG.

The remainder of the paper is organized as follows: Section 2 describes the measurement setup and the acquisition/processing techniques. The results for HR, HRV, and time intervals related analyses are reported in Section 3. Finally, the authors provide their conclusions in Section 4.

2. Materials and methods

The experimental tests were conducted at Università Politecnica delle Marche in compliance with the principles outlined in the WMA declaration of Helsinki [23]. Four different measurement methods were employed, namely Electrocardiography, Photoplethysmography, Phonocardiography, and Vibrocardiography. All the signals were simultaneously acquired in rest conditions.

2.1. Measurement setup

A schematic view of the measurement setup is reported in Figure 1. The subject was laying supine, as still as possible to minimize motion artifacts. The following sensors were positioned:

- 3-lead ECG (MLA2540, ADInstruments, New Zealand).
- PCG sensor (MLT201, ADInstruments, New Zealand).
- Laser Doppler vibrometer for VCG acquisition (PDV 100, Polytec GmbH, Germany).
- PPG sensor (Pulse Amped Sensor, World Famous Electronics llc., USA).

The measurement devices were connected to a 16-bit A/D acquisition board (A/D board n.1, PowerLab 4/25, ADInstruments, New Zealand) and to a second A/D acquisition board (A/D board n.2, NI 6008, National instruments, Texas, USA).

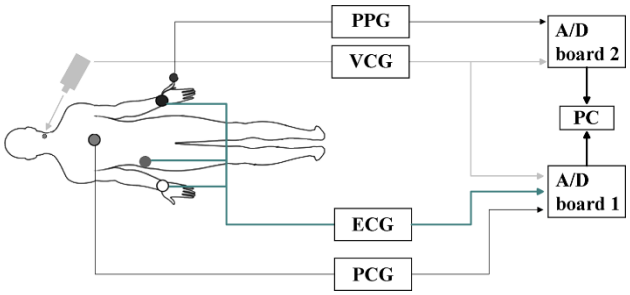

Figure 1. Schematic view of the measurement setup.

The ECG electrodes were applied on the left and right wrists and on the hip bone (neutral electrode) of the subject. The PCG microphone head was placed on the thorax in correspondence of the heart apex and fixed with a sticking plaster to minimize movements. The VCG measurement beam was directed in correspondence of the carotid sinus and the optical was placed on a tripod at a distance of approximately 1 m from the subject, perpendicularly to the skin (which was treated with a hydrating lotion, 45% zinc oxide, to maximize reflectivity and enhance signal-to-noise ratio). Finally, the PCG transducer was positioned on the left thumb. The ECG and PCG sensors were connected to the A/D board 1, while the PPG sensor was connected to the A/D board 2. The VCG sensor was connected to both the boards for synchronization purposes. All the measurement signals were sampled at 1 kHz and no further digital filters were applied on the raw signals except for the anti-aliasing filter integrated in both the acquisition boards.

2.2. Test protocol

The test population consisted in 26 healthy subjects (10 males and 16 females, aged 23±2 years – the demographic details are reported in Table 1), who were recruited on a voluntary basis. They were made sign an informed consent module after the study objective and methods were clearly explained to them. Two different types of tests were made on each subject:

- n. 4 repeated 60-s recordings.
- n. 1 single 6-min recording (for HRV analysis).

Table 1. Participants' demographic characteristics (data are reported as mean±standard deviation).

Age [years]	Weight [kg]	Height [m]	BMI [kg/m^2]
23±2	64±13	1.71±0.08	21.86±3.09

After a settling time of approximately 60 s, necessary to let the subject relax, the acquisition was started.

2.3. Data processing

The acquired raw signals were pre-processed to remove the DC component and noise. A 3rd order Butterworth digital band-pass filter was applied, selecting the following cut-off frequencies:

- ECG signal: 0.8-20 Hz.
- PPG signal: 0.8-5 Hz.
- VCG signal: 4-6 Hz.
- PCG signal: 15-25 Hz. Being the frequency content higher with respect to the other signals, these cut-off frequencies were chosen to highlight the characteristics morphologically comparable to the ECG ones, i.e., S1 (related to R-peak in ECG) and S2 (delayed with respect to S1) sounds. The other sounds (i.e., S3 and S4 – with lower amplitude) cannot be detected essentially due to the acquisition hardware. Hence, PCG signal was enveloped to extract the features of interest [22].

An example of the filtered ECG signal is reported in Figure 2. Then, all the signals were normalized.

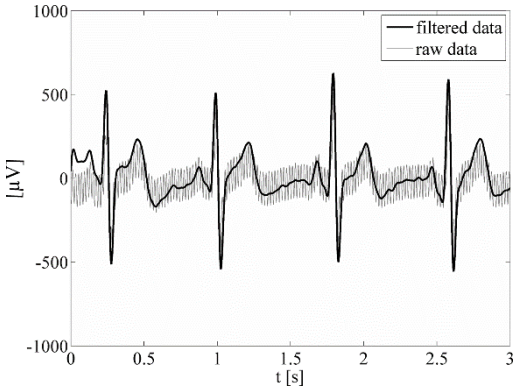

Figure 2. Effect of the band-pass filter (black) on the ECG raw (grey) signal, before normalization.

The first parameter extracted from each of the four signals was HR [21], expressed in beat-per-minutes (bpm), representing the mean cardiac frequency over the 60 s observation period, as reported in Equation (1):

$$HR = \frac{1}{HP\ [s]} * 60\ [\text{bpm}] \quad (1)$$

where HP is the Heart Period, computed as the time interval between two consecutive periodic features in each signal (i.e., R-peak for ECG, S1-sound for PCG, P1-peak for PPG, and V1-peak for VCG).

For the uncertainty estimation, the HR values measured from PCG, PPG, and VCG were compared to the ones simultaneously measured from the ECG (gold standard), in terms of linear regression, Pearson's correlation coefficient, and R^2 value.

As a second parameter, the time duration of each cardiac event (measured in ms) was calculated for HRV analysis in time domain. Hence, the tachogram (i.e., the sequence of all the time intervals between two consecutive main features) was computed for each of the four sensors [24] and different HRV statistics parameters were calculated [21,25,26] (Figure 3):

- RRmax: maximum cardiac period [ms].
- RRavg: mean cardiac period [ms].
- RRmin: minimum cardiac period [ms].
- STD: standard deviation of the time intervals between the main peaks [ms].
- NN50: number of consecutive time intervals with a difference greater than 50 ms.
- pNN50: percentage of the NN50 on the total amount of the time intervals [%].
- RMSSD: root mean square of the time intervals between the main peaks [ms].

Also, the Poincaré plot [30] was used to analyse the HRV in the time domain. It reports each time interval versus the previous one. The indices calculable from Poincaré plot (Figure 4) are the following ones [27,28]:

- SD1: standard deviation of the samples along the minor axis of the plot [ms].
- SD2: standard deviation of the samples along the major axis of the plot [ms].

- SD12: ratio of SD1 against SD2.
- SDRR: standard deviation of Heart Period (HP) [ms].
- S: area of the ellipse fitting the points [ms^2].

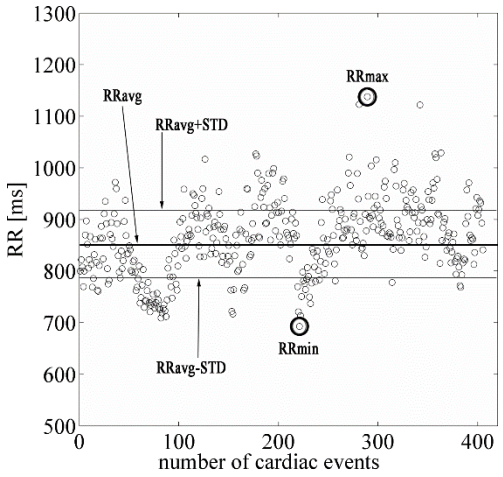

Figure 3. Example of tachogram, obtained from the proposed method applied to the ECG signal.

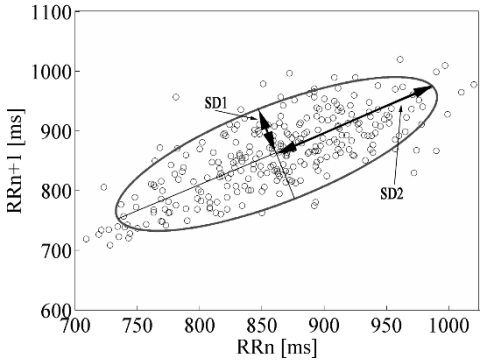

Figure 4. Example of Poincaré plot, obtained from the proposed method applied to the ECG signal.

All the parameters listed above were compared between test signals (PCG, VCG, and PPG) and reference signal (i.e., ECG). The results were discussed in terms of 95% Confidence Interval (CI).

Moreover, other relevant cardiac features were measured in the different types of signals, in order to evaluate their correlation to the QT interval; in particular, the authors considered four time intervals in PCG signal, three in VCG, and one in PCG, as it will be described in detail in the next section. Finally, the Bland-Altman plot-based analysis [29] was performed.

3. Results

The data analyses covered the following aspects:

- Computation of HR, from the different types of signals (i.e., ECG, PCG, PPG, and VCG) and evaluation of measurement accuracy with respect to reference data (i.e., ECG).
- Measurement of HRV time domain parameters and comparison with reference data.
- Identification of characteristic points and measurement of the QT related time intervals from PPG and VCG signals and comparison with reference data.

Results and considerations regarding these items are reported below.

3.1. Heart rate assessment

The performance of the adopted approach was demonstrated to be comparable to traditional algorithm (i.e., Pan & Tompkins) [20]. The mean values of HR, computed for the PPG, PCG, and VCG signals for each subject, together with their percentage deviation with respect to the gold standard (i.e., ECG derived HR), are reported in Table 2. The HR measurement is accurate for all the considered sensors, since the percentage deviation is always <0.30%. The maximum deviation is 4.29 bpm (i.e., 4.74%) obtained for PCG (subject 3). Considering the mean performance values, the minimum percentage deviation is achieved for VCG (-0.11%); similarly, for PCG the mean percentage deviation is 0.14% (hence, similar in absolute terms).

Then, the uncertainty was estimated comparing the tachograms heartbeat per heartbeat. In particular, the percentage deviation was computed as the ratio of the HR difference between test (i.e., PPG, PCG, and VCG) and reference (i.e., ECG) signals.

Table 2. HR [bpm] computation from different sensors and percentage deviation (σ (%)) with respect to gold standard (ECG).

Subject	HR (ECG)	HR (PPG)	Dev. (%)	HR (PCG)	Dev. (%)	HR (VCG)	Dev. (%)
1	53.95	54.18	0.41	53.03	-1.71	53.60	-0.53
2	63.34	63.25	-0.14	63.32	-0.03	63.31	-0.05
3	90.56	90.53	-0.03	86.27	-4.74	90.53	-0.03
4	70.85	70.85	-0.01	70.66	-0.28	70.73	-0.18
5	62.50	62.50	-0.01	62.48	-0.04	63.06	0.87
6	68.40	68.67	0.39	69.28	1.28	67.93	-0.68
7	61.71	62.27	0.89	60.97	-1.21	61.74	0.05
8	64.98	64.76	-0.36	64.26	-1.11	64.27	-1.11
9	70.74	70.81	0.10	70	-1.05	70.29	0.34
10	80.64	80.68	0.05	80.65	0.01	80.30	-0.36
11	70.23	70.24	0.02	70.19	-0.05	70.05	-0.26
12	66.10	66.09	-0.01	66.14	0.07	66.28	0.27
13	59.98	59.91	-0.12	59.96	-0.03	59.90	-0.13
14	90.13	90.16	0.03	90.64	0.57	89.84	-0.32
15	56.75	56.80	0.08	57.1	0.61	56.75	0.03
16	77.59	77.61	0.03	77.12	-0.61	77.31	-0.36
17	72.87	73.94	1.50	72.91	0.05	72.67	-0.27
18	88.92	88.96	0.05	91.43	2.83	89.18	0.30
19	73.06	73.02	-0.06	72.97	-0.12	73.39	0.46
20	57.88	57.86	-0.04	57.9	0.04	57.68	-0.34
21	67.03	67.20	0.26	66.36	-1.00	67.08	0.07
22	85.34	85.40	0.07	85.39	0.06	84.68	-0.75
23	75.68	75.67	-0.02	75.67	-0.02	75.80	0.16
24	77.07	77.06	-0.02	77.02	-0.07	77.68	0.83
25	72.22	72.64	0.59	71.67	-0.76	71.62	0.18
26	66.65	66.66	0.03	66.37	-0.42	67.53	1.34
Mean			**0.14**		**-0.30**		**-0.11**

The correlation between test and reference signals, as well as the statistics of the measurement differences (i.e., residuals), are reported in Table 3. Sensitivity and bias were obtained as the angular coefficient (i.e., slope) and the y-axis intercept of the interpolating curve (i.e., calibration line). The strength of the correlation was assessed through R^2 and Pearson's correlation coefficient. Finally, after the calibration procedure (an example is reported in Figure 5), the authors evaluated the measurement uncertainty [30] (in bpm) through the analysis of measurement differences (e.g., the normalized

residuals distribution for PPG sensor is reported in Figure 6, proving that the measured data are Gaussian). Also, the expanded uncertainty (coverage factor k=2) was computed. It is possible to observe that PPG is the most accurate measurement method, quickly followed by VCG. It is important to note that PPG is a contact measurement method, suffering from movement artefacts, whereas VCG is operated without any contact with the subject (measurement distance of approximately 1 m), representing an advantage in certain operating conditions.

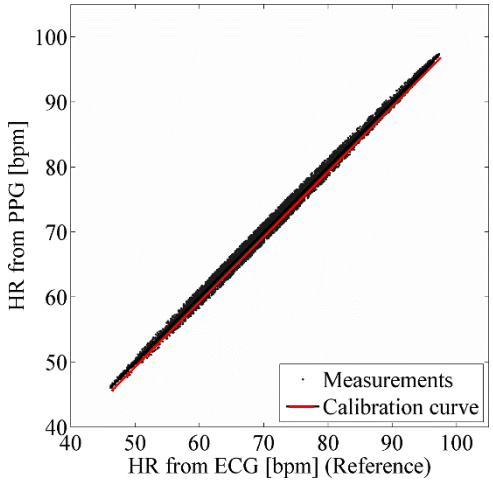

Figure 5. Measurements (black points) and calibration curve (red line) between HR computed from PPG and ECG signals, respectively.

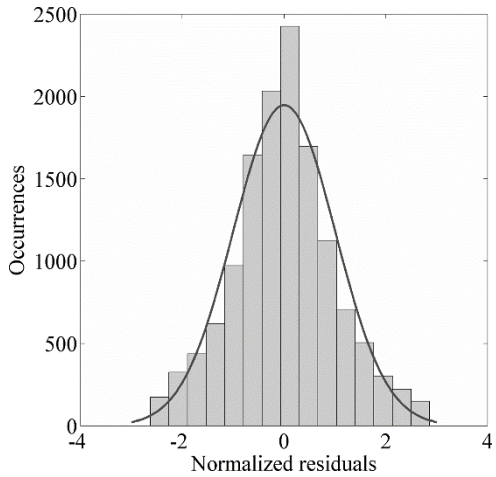

Figure 6. PPG signal: distribution of the residuals for HR.

Table 3. Correlation and residuals relative to PCG, PPG and VCG sensors (Sens., sensitivity of the calibration curve or angular coefficient; mean dev., mean deviation; 2*σ, expanded uncertainty).

Sensor	Sens.	Bias [bpm]	Pearson	R^2	Mean dev. [bpm]	2*σ [bpm]
PCG	0.998	0.382	0.992	98.4	<0.01	2.5
PPG	1.002	-0.128	0.998	99.7	<0.01	1.2
VCG	1.003	-0.158	0.997	99.4	<0.01	1.6

3.2. Heart rate variability

HRV analysis has been conducted in the time domain for PPG and VCG signals.

The mean values and the 95% CI [31] for each parameter derived from the tachogram (i.e., RRmax, RRavg, RRmin, STD, NN50, pNN50) are reported in Figure 7 and Figure 8 for PPG and VCG signals,

respectively. Similarly, the parameters derived from Poincaré plot are reported in Figure 9 and Figure 10 for PPG and VCG signals, respectively. The use of the interpolating lines (reported in Table 3) allows us to remove the bias and to obtain more accurate results (no statistical differences reported for the calibrated data), both for PPG and VCG sensors. This suggests that other useful parameters can be provided by physiological waveforms different from ECG to describe the overall health status of a subject.

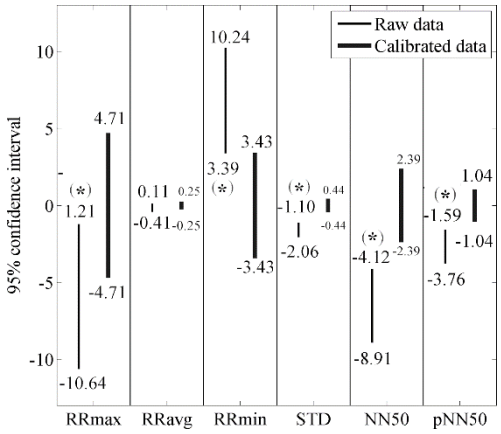

Figure 7. Confidence intervals for HRV parameters (tachogram) extracted from PPG signals.

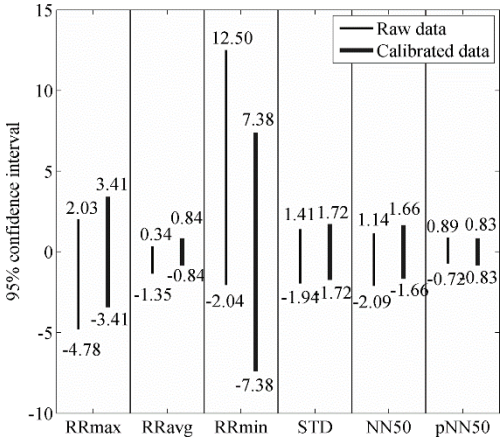

Figure 8. Confidence intervals for HRV parameters (tachogram) extracted from VCG signals.

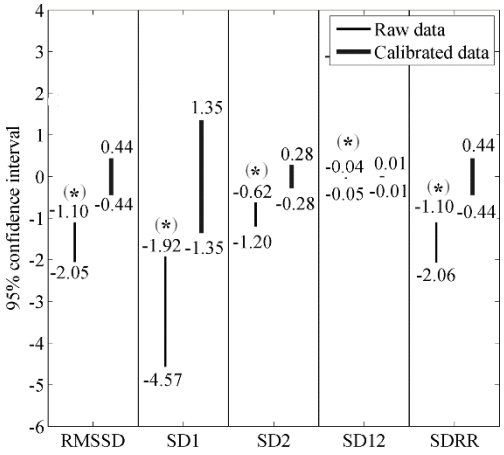

Figure 9. Confidence intervals for HRV parameters (Poincaré plot) extracted from PPG signals.

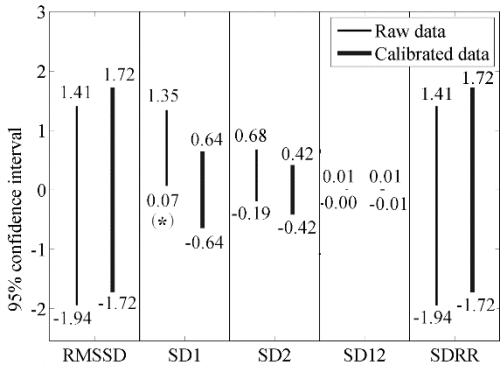

Figure 10. Confidence intervals for HRV parameters (Poincaré plot) extracted from VCG signals.

3.3. Identification of signals characteristic points and measurement of QT related time intervals

The analysis of the ECG waveform by the proposed algorithm [26] allowed us to precisely identify all the typical ECG features (i.e., P, Q, R, S, T points, duration of QRS complex, and offset of T-wave – see Figure 11). Therefore, is possible to identify the time intervals of ECG trace and to verify the possibility to measure the same time intervals also from the other sensors.

With regard to PCG signal, the physiological significance of S1 and S2 sounds is well acknowledged [22]; in fact, they are related to the closure of mitral and tricuspid valves at the start of systole (S1) and to the closure of the aortic and pulmonic valves at the end of systole (S2). With the proposed signal processing method [21], it was possible to clearly identify both the two sounds in the measured signal (Figure 12).

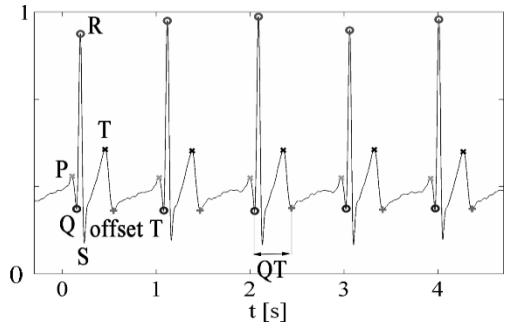

Figure 11. ECG signal with characteristic waveform points.

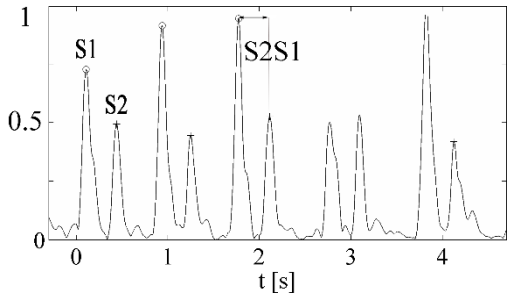

Figure 12. PCG signal (normalized) with the identification of the S1 and S2 sounds.

VCG and PPG are mechanical-related signals and the significance of their morphology has not been ascertained yet, even if their stationarity are confirmed [32–34]. Consequently, the authors computed several intervals by identifying all the peaks characterizing PPG and VCG waveforms and evaluate the possible correlation with the ECG derived QT interval. Figures 13 and 14 show the located points for PPG (i.e., P1, P2, P3, P4, and P5) and VCG (i.e., V1, V2, V3, V4, and V5) signals, respectively, and the considered time intervals. Hence, the measurement differences between these intervals and the QT interval from ECG were evaluated; in particular, the authors considered the following time intervals (see Table 4):

- S2S1 for PCG.
- P3P1, P4P1, P3P0, and P4P2 for PPG.
- V2V1 and V2V3 for VCG.

The differences with respect to QT were computed to obtain the bias as their mean value. Hence, the standard deviation of residuals was computed to estimate the measurement uncertainty. The percentage uncertainty was obtained dividing the standard deviation of the residuals by the reference value and multiplying the results by 100.

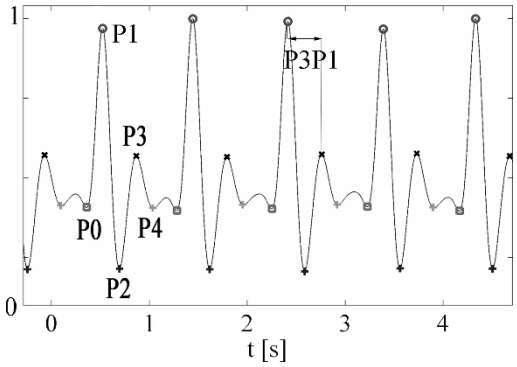

Figure 13. normalized PPG signal with identified peaks and related time intervals (P3P1).

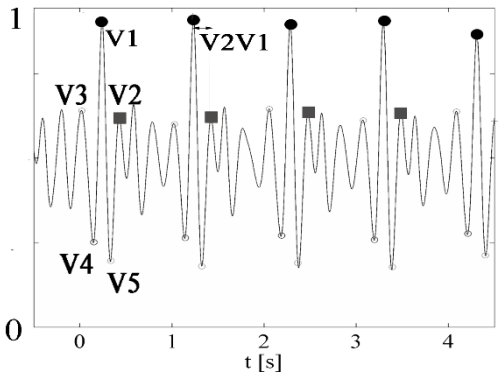

Figure 14. Normalized VCG signal with identified peaks and related time intervals (V2V1).

As it can be observed in Table 4, the uncertainties of S2S1, P3P1, and V2V1 intervals with respect to the reference QT cannot be disregarded. This aspect deserves to be further investigated to evaluate the possibility of determining such an important cardiac parameter from minimally intrusive measurement methods (PPG and PCG), as well as from a fully non-contact method, i.e., VCG.

Table 4. Average offset and final uncertainty related to PCG, PPG, and VCG sensors in QT-related features (QT value from ECG = 466±77 ms, reported as mean±1.96*standard deviation).

Feature	Mean Bias [ms]	Uncertainty [%]
S2S1	-89.8	**±10.9**
P3P1	-127.4	**±16.8**
P4P1	34.7	±22.7
P3P0	46.2	±24.5
P4P2	-144.5	±42.4
V2V1	-250.1	**±10.9**
V2V3	-74.8	±14.3
V2V4	-165.0	±11.9

Differently from the HR computation, several issues occurring during acquisition and processing of the signals affect the overall quality of this type of analysis. In fact, the inter-subject variability plays a fundamental role: physical constitution (e.g., fat tissue concentration), peripheral blood circulation, presence of nail polish, laser spot positioning, filtering methods, and other test procedure related matters modify the acquired pattern of PCG, PPG, and VCG signals. Each subject's signals present a different calibration curve, so that it is not possible to obtain a relationship valid for the whole population. The uncertainty can be reduced by computing a personal calibration curve, rather than one for all subjects. Sensitivity (m) and bias (b) parameters of the calibration lines for subjects 1, 2, and 3 are reported in Table 5 together with percentage expanded uncertainty (k=2) related to the QT assessment from VCG using personal calibration lines applied to V2V1 intervals data.

Table 5. Calibration curves between V2V1 and QT on three subjects.

Subject	m	b [ms]	Uncertainty [%]
1	0.48	-272	±2.6
2	1.13	-524	±2.2
3	0.15	-99	±4.3

In this way, the uncertainty is significantly reduced (< ±4.3%). In figure 15, the Bland-Altman plot related to subject 1 is reported.

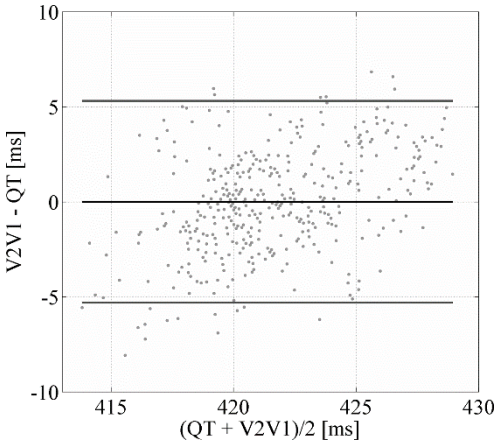

Figure 15. Bland-Altman plot: measure of QT interval by V2V1 interval (subject 1).

4. Conclusions

The algorithm proposed in [19] is able to accurately identify the main reference points in ECG waveform, with performances comparable to traditional algorithm (i.e., P&T [15]). In [21], the use of the algorithm was extended to other measurement methods (i.e., PPG, PCG, and VCG). In the present work, the analysis of the data gathered in an extended measurement campaign (test population of 26 subjects) demonstrated the algorithm robustness not only for HR measurement, but also for HRV analysis and waveform time intervals.

Regarding the measurement of HR, results show measurement differences of ±2.5 bpm, ±1.2 bpm, and ±1.6 bpm for PCG, PPG, and VCG sensors with respect to ECG (i.e., gold standard). Concerning HRV, the analysis was focused on the possibility to use PPG (contact sensor) and VCG (contactless technique) signals to operate. The authors have applied the Student's t-test and reported its graphical representation through 95% CI to underline possible statistically differences between HRV parameters computed from PPG/VCG (i.e., test signals) with respect to the gold standard (i.e., ECG). The bias, whenever present, can be removed through appropriate calibration coefficients. The 95% CI computed for all the considered measurement methods after the calibration and adjustment procedures do not present statistical differences with respect to the standard technique, hence the results can be considered accurate. This suggests that the adopted processing procedure can be applied also to such measurement methods to assess physiological information of clinical relevance other than HR.

Finally, the authors investigated the agreement between QT (computed from ECG) and other time intervals from the other considered sensors. At first, each waveform was characterized according to its morphology. As regards PCG, S1 and S2 (with acknowledged clinical significance) were considered; for both PPG and VCG, five points were identified. Among different measured time intervals, those which provided a better agreement with QT were S2S1 interval for PCG (uncertainty < ±10.9%), P3P1 interval for PPG (uncertainty < ±16.8%), and V2V1 interval for VCG (uncertainty < ±10.9%). These results were obtained on the whole population, using a single calibration line, but many issues (e.g., physical constitution, peripheral blood circulation, presence of nail polish, laser spot positioning, and filtering method) undoubtedly affect them. In fact, if a personal calibration line is used, uncertainty can be reduced (< ±4.3%). This would make it possible to obtain a valid measure of a time interval in agreement with the reference QT also by means of a non-contact method (i.e., VCG).

In conclusion, the proposed measurement procedure, adequately fine-tuned for the subject under test, can be applied to signals of different nature to extract a lot of useful information, also indirectly (e.g., the respiration rate).

Future works could be focused on the identification of a standardized acquisition procedure, to minimize the effects of possible artifacts. In particular, for VCG signal the integration of a thermal camera in the test setup could be used to accurately identify the optimum laser spot location above a blood vessel.

Moreover, the adopted data processing approach could be successfully integrated in real-time systems, such as ECG analyzers [35]. Furthermore, the capability of this algorithm to accurately extract relevant features could support existent techniques in the field of biometrics and person identification by means of ECG signals analysis [36,37].

References

[1] F. Desai, D. Chowdhury, R. Kaur, M. Peeters, R.C. Arya, G.S. Wander, S.S. Gill, R. Buyya, HealthCloud: A system for monitoring health status of heart patients using machine learning and cloud computing, Internet of Things. 17 (2022) 100485. https://doi.org/10.1016/J.IOT.2021.100485.

[2] P. Revanthsai, N.S. Maadhurya, S.D.V. Konijeti, B.K. Priya, A foundational model to spot indications of generalized anxiety disorder and assist mental well being, in: J. Phys. Conf. Ser., IOP Publishing, 2022: p. 12031.

[3] L. Scalise, L. Casacanditella, G. Cosoli, Measuring the human psychophysiological conditions without contact, in: J. Phys. Conf. Ser., 2017. https://doi.org/10.1088/1742-6596/882/1/012016.

[4] V.N. Varghees, H. Cao, L. Peyrodie, Variational Mode Decomposition-Based Simultaneous R Peak Detection and Noise Suppression for Automatic ECG Analysis, IEEE Sens. J. 23 (2023) 8703–8713. https://doi.org/10.1109/JSEN.2023.3257332.

[5] G. Cosoli, A. Poli, L. Antognoli, S. Spinsante, L. Scalise, What is my heart rate right now? Comparing data from different devices, in: 2022 IEEE Int. Instrum. Meas. Technol. Conf., Ottawa, 2022: p. (accepted for publication).

[6] J. Kranjec, S. Beguš, G. Geršak, J. Drnovšek, Non-contact heart rate and heart rate variability measurements: A review, Biomed. Signal Process. Control. 13 (2014) 102–112. https://doi.org/10.1016/J.BSPC.2014.03.004.

[7] J. Kranjec, S. Begus, J. Drnovsek, G. Gersak, Novel methods for noncontact heart rate measurement: A feasibility study, IEEE Trans. Instrum. Meas. 63 (2014) 838–847. https://doi.org/10.1109/TIM.2013.2287118.

[8] M.C. Faisant, J. Fontecave-Jallon, B. Genoux, B. Rivet, N. Dia, M. Resendiz, D. Riethmuller, V. Equy, P. Hoffmann, Non-invasive fetal monitoring: Fetal Heart Rate multimodal estimation from abdominal electrocardiography and phonocardiography, J. Gynecol. Obstet. Hum. Reprod. 51 (2022) 102421. https://doi.org/https://doi.org/10.1016/j.jogoh.2022.102421.

[9] H. Kinnunen, A. Rantanen, T. Kentt, H. Koskim ki, Feasible assessment of recovery and cardiovascular health: Accuracy of nocturnal HR and HRV assessed via ring PPG in comparison to medical grade ECG, Physiol. Meas. 41 (2020). https://doi.org/10.1088/1361-6579/AB840A.

[10] S. Knight, J. Lipoth, M. Namvari, C. Gu, M. Hedayati, S. Syed-Abdul, R.J. Spiteri, The Accuracy of Wearable Photoplethysmography Sensors for Telehealth Monitoring: A Scoping Review, Https://Home.Liebertpub.Com/Tmj. 29 (2023) 813–828. https://doi.org/10.1089/TMJ.2022.0182.

[11] S. Casaccia, E.J. Sirevaag, E. Richter, J.A. O'Sullivan, L. Scalise, J.W. Rohrbaugh, Decoding carotid pressure waveforms recorded by laser Doppler vibrometry: Effects of rebreathing, AIP Conf. Proc. 1600 (2014) 298–312. https://doi.org/10.1063/1.4879596.

[12] G. Cosoli, L. Casacanditella, E.P. Tomasini, L. Scalise, Evaluation of heart rate variability by means of laser doppler vibrometry measurements, in: J. Phys. Conf. Ser., 2015. https://doi.org/10.1088/1742-6596/658/1/012002.

[13] E. Lepeschkin, B. Surawicz, The Measurement of the Q-T Interval of the Electrocardiogram, (n.d.). http://ahajournals.org (accessed August 22, 2023).

[14] A.J. Camm, M. Malik, J.T. Bigger, G. Breithardt, S. Cerutti, R.J. Cohen, P. Coumel, E.L. Fallen, H.L. Kennedy, R.E. Kleiger, Heart rate variability: standards of measurement, physiological interpretation and clinical use. Task Force of the European Society of Cardiology and the North American Society of Pacing and Electrophysiology, Circulation. 93 (1996) 1043–1065.
[15] J. Pan, W.J. Tompkins, A Real-Time QRS Detection Algorithm, IEEE Trans. Biomed. Eng. BME-32 (1985) 230–236. https://doi.org/10.1109/TBME.1985.325532.
[16] K. Zhao, Y. Li, G. Wang, Y. Pu, Y. Lian, A robust QRS detection and accurate R-peak identification algorithm for wearable ECG sensors, Sci. China Inf. Sci. 64 (2021) 1–17. https://doi.org/10.1007/S11432-020-3150-2/METRICS.
[17] S.K. Mukhopadhyay, S. Krishnan, Robust identification of QRS-complexes in electrocardiogram signals using a combination of interval and trigonometric threshold values, Biomed. Signal Process. Control. 61 (2020) 102007. https://doi.org/10.1016/J.BSPC.2020.102007.
[18] M.B. Hossain, S.K. Bashar, A.J. Walkey, D.D. McManus, K.H. Chon, An Accurate QRS Complex and P Wave Detection in ECG Signals Using Complete Ensemble Empirical Mode Decomposition with Adaptive Noise Approach, IEEE Access. 7 (2019) 128869–128880. https://doi.org/10.1109/ACCESS.2019.2939943.
[19] X. Hu, J. Liu, J. Wang, Z. Xiao, J. Yao, Automatic detection of onset and offset of QRS complexes independent of isoelectric segments, Measurement. 51 (2014) 53–62. https://doi.org/10.1016/J.MEASUREMENT.2014.01.011.
[20] S. Mitra, M. Mitra, B.B. Chaudhuri, A Rough-Set-Based Inference Engine for ECG Classification, IEEE Trans. Instrum. Meas. 55 (2006) 2198–2206. https://doi.org/10.1109/TIM.2006.884279.
[21] G. Cosoli, L. Casacanditella, F. Pietroni, A. Calvaresi, G.M. Revel, L. Scalise, A novel approach for features extraction in physiological signals, 2015 IEEE Int. Symp. Med. Meas. Appl. MeMeA 2015 - Proc. (2015) 380–385. https://doi.org/10.1109/MEMEA.2015.7145232.
[22] H. Naseri, M.R. Homaeinezhad, Detection and boundary identification of phonocardiogram sounds using an expert frequency-energy based metric, Ann. Biomed. Eng. 41 (2013) 279–292. https://doi.org/10.1007/S10439-012-0645-X/FIGURES/11.
[23] WMA Declaration of Helsinki – Ethical Principles for Medical Research Involving Human Subjects – WMA – The World Medical Association, (n.d.). https://www.wma.net/policies-post/wma-declaration-of-helsinki-ethical-principles-for-medical-research-involving-human-subjects/ (accessed December 9, 2020).
[24] H.F. Posada-Quintero, D. Delisle-Rodríguez, M.B. Cuadra-Sanz, R.R. Fernández de la Vara-Prieto, Evaluation of pulse rate variability obtained by the pulse onsets of the photoplethysmographic signal., Physiol. Meas. 34 (2013) 179–187. https://doi.org/10.1088/0967-3334/34/2/179.
[25] L. Scalise, U. Morbiducci, Non-contact cardiac monitoring from carotid artery using optical vibrocardiography, Med. Eng. Phys. 30 (2008) 490–497. https://doi.org/10.1016/J.MEDENGPHY.2007.05.008.
[26] L. Hejjel, E. Roth, What is the adequate sampling interval of the ECG signal for heart rate variability analysis in the time domain?, Physiol. Meas. 25 (2004) 1–7. https://doi.org/10.1088/0967-3334/25/6/006.
[27] P.W. Kamen, A.M. Tonkin, Application of the Poincaré plot to heart rate variability: a new measure of functional status in heart failure., Aust. N. Z. J. Med. 25 (1995) 18–26. https://doi.org/10.1111/j.1445-5994.1995.tb00573.x.
[28] C.M.A. van Ravenswaaij-Arts, L.A.A. Kollee, J.C.W. Hopman, G.B.A. Stoelinga, H.P. van Geijn, Heart rate variability, Ann. Intern. Med. 118 (1993) 436–447.
[29] J.M. Bland, D.G. Altman, STATISTICAL METHODS FOR ASSESSING AGREEMENT BETWEEN TWO METHODS OF CLINICAL MEASUREMENT, (n.d.).

[30] JCGM, Evaluation of measurement data-Guide to the expression of uncertainty in measurement Évaluation des données de mesure-Guide pour l'expression de l'incertitude de mesure, (2008). www.bipm.org (accessed September 2, 2022).
[31] B.R. Kirkwood, J.A.C. Sterne, Essential medical statistics, John Wiley & Sons, 2010.
[32] H.K. Walker, W.D. Hall, J.W. Hurst, Clinical methods: the history, physical, and laboratory examinations, (1990).
[33] A.A. Alian, K.H. Shelley, Photoplethysmography, Best Pract. Res. Clin. Anaesthesiol. 28 (2014) 395–406. https://doi.org/10.1016/J.BPA.2014.08.006.
[34] F. Bousefsaf, C. Maaoui, A. Pruski, Continuous wavelet filtering on webcam photoplethysmographic signals to remotely assess the instantaneous heart rate, Biomed. Signal Process. Control. 8 (2013) 568–574. https://doi.org/10.1016/J.BSPC.2013.05.010.
[35] G. Lamarque, P. Ravier, C. Dumez-Viou, A new concept of virtual patient for real-time ECG analyzers, IEEE Trans. Instrum. Meas. 60 (2010) 939–946.
[36] A.D.C. Chan, M.M. Hamdy, A. Badre, V. Badee, Wavelet distance measure for person identification using electrocardiograms, IEEE Trans. Instrum. Meas. 57 (2008) 248–253.
[37] A. Pantanowitz, A. Ahmed Aleidan, Q. Abbas, Y. Daadaa, I. Qureshi, G. Perumal, M.E. A Ibrahim, A.E. S Ahmed, Biometric-Based Human Identification Using Ensemble-Based Technique and ECG Signals, Appl. Sci. 2023, Vol. 13, Page 9454. 13 (2023) 9454. https://doi.org/10.3390/APP13169454.